CHAPTER 3

IN-SILICO IDENTIFICATION OF WITHANOLIDE A AS A NEUROPROTECTANT

Chapter Highlights

- ***Analysis of drug like properties of Withania somnifera phytochemicals***
- ***Molecular docking simulation of W. somnifera phytochemicals against PARP-1 using Auto Dock Tools 1.5.6***
- ***Analysis of binding patterns of the phytochemicals and comparison with the reported inhibitors of PARP-1***

ABSTRACT

Poly (ADP-ribose) polymerase-1 (PARP-1) reverses DNA damage by repairing DNA nicks and breaks in the normal cellular environment. However, during abnormal conditions like cerebral ischemia and other neurological disorders, overactivation of PARP-1 leads to neuronal cell death via a caspase-independent programmed cell death pathway. Strategies involving inhibition or knockout of PARP-1 have proved beneficial in combating neuro-cytotoxicity. In this study we performed in-silico analysis of 27 phytochemicals of *Withania somnifera* (*Ashwagandha*), to investigate their inhibition efficiency against PARP-1. Out of 27 phytochemicals, we report 12 phytochemicals binding to the catalytic domain of PARP-1 with an affinity higher than FR257517, PJ34 and Talazoparib (highly potent inhibitors of the enzyme). Among these 12 compounds, five phytochemicals namely Stigmasterol, Withacnistin, Withaferin A, Withanolide G and Withanolide A show an exceptionally high binding affinity for the catalytic domain of PARP-1 and bind to the enzyme with similar hydrogen bond formation and hydrophobic interaction pattern as their inhibitors. All of these

phytochemicals follow Lipinski's rule of 5 so they can be further developed into potential future neuro-therapeutic drugs against neurodegenerative disorders involving neuronal cell death.

3.1. INTRODUCTION

Neuronal damage occurring during neurodegenerative diseases, hypoxia, ischemia, and infections involves a specially choreographed cell death pathway exhibiting characteristics of both necrosis and apoptosis [1]. Among various factors participating in the execution of this pathway, deoxyribose nucleic acid (DNA) repair enzyme poly (ADP-ribose) polymerase-1 (PARP-1) plays a significant role [2]. Excessive formation of peroxynitrite during neurotoxicity leads to extensive DNA damage, causing over-activation of PARP-1 which undertakes the responsibility of DNA repair [2, 3]. In its attempt to repair damaged DNA, PARP-1 often triggers cell death via a cascade of events involving depletion of the cellular energy store by depreciating nicotinamide adenine dinucleotide (NAD^+) and adenosine triphosphate (ATP) storage of cell [4-6]. The role of PARP-1 in caspase-independent programmed cell death is illustrated in Fig. 3.1. PARP-1 is also reported to act directly on mitochondria and mediate peroxynitrite-induced mitochondrial damage [7]. PARP-1 also initiates translocation of apoptosis inducing factor (AIF), an established contributor of caspase-independent neuronal cell death, from mitochondria to nucleus [8, 9]. AIF mediated apoptotic cell death is reported in cerebral ischemia and in excitotoxic conditions which cause mitochondrial membrane disruption [10-12]. AIF acts downstream in PARP-1 dependent cell death [11] and is activated by ADP-ribose polymers (PARs) formed as a by-product of PARP-1 activation [8]. PARs can also inhibit histones, DNA polymerases, topoisomerases I and II as well as PARP-1 itself by poly-ADP-ribosylation, thus inhibiting their activity [13]. Inhibition

of PARP-1 provides neuroprotection in ischemia-reperfusion injury [14], reactive oxygen species-induced injury [15], and glutamate excitotoxicity [11], Alzheimer's disease (AD) [16] and Parkinson's disease [17]. Targeting of PARP-1, to inhibit cell death is a well-adopted strategy in cancer research and rigorous research has identified Talazoparib as a bioavailable PARP-1 inhibitor. This compound has successfully entered phase III clinical trial for the treatment of breast cancer [18-20].

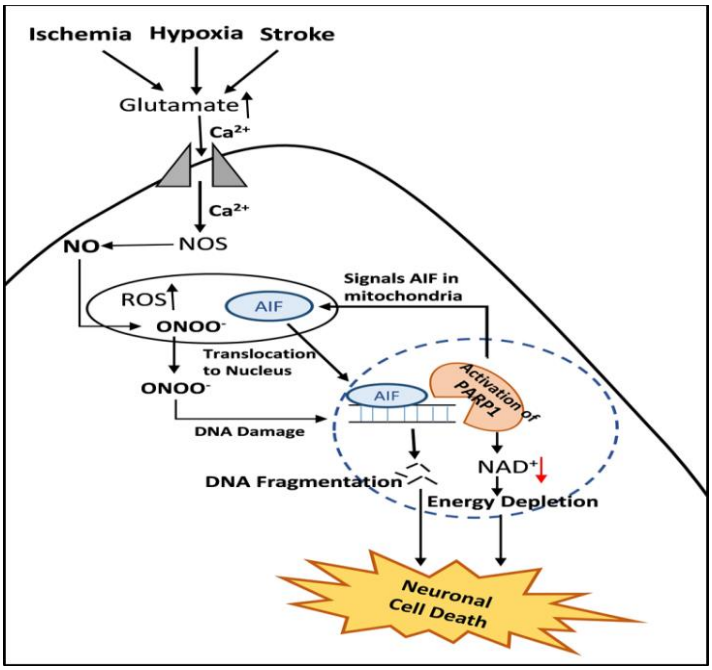

Fig. 3.1.: PARP-1 plays a pivotal role in caspase-independent cell death by recruiting AIF and depleting cell energy reservoir [4, 5].

The present study focuses on identifying possible inhibitors of PARP-1 from phytochemicals present in *Withania somnifera* (*Ashwagandha),* a traditional Indian herb widely noted for its neuro protective potential [21-24] and compares their inhibition potency with known PARP-1 inhibitors 2-{3-[4-(4-fluorophenyl)-3,6-dihydro-1(2H)-pyridinyl]propyl}-8-methyl-4(3H)-quinazolinone (FR257517) (Fig 3.2.a), 2-(dimethylamino)-N-(6-oxo-5,6-dihydrophenanthridin-2-yl)acetamide (PJ34) (Fig. 3.2.b) and Talazoparib (Fig. 3.2.c), for the

development of plausible future strategies to combat with neurotoxicity and neurodegeneration.

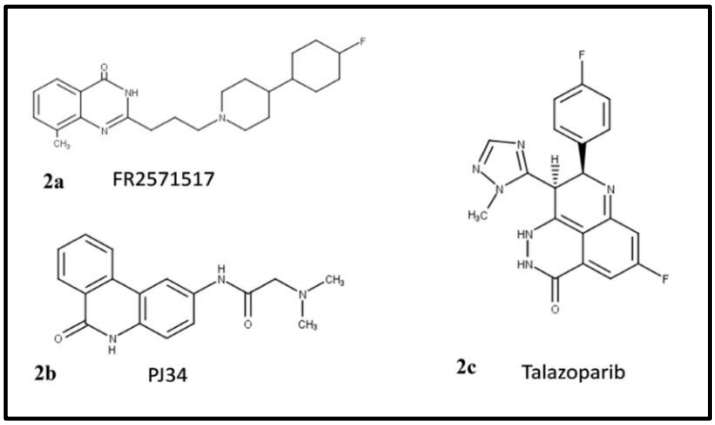

Fig. 3.2: Structures for known PARP-1 inhibitors. (3.2.a) 2-{3-[4-(4-fluorophenyl)-3,6-dihydro-1(2H)-pyridinyl]propyl}-8-methyl-4(3H)-quinazolinone (FR257517), (3.2.b) 2-(dimethylamino)-N-(6-oxo-5,6-dihydrophenanthridin-2-yl)acetamide (PJ34), (3.2.c) Talazoparib.

3.2. MATERIALS AND METHOD

3.2.1. Selection and preparation of inhibitors

W.somnifera (WS) phytochemicals used for this study were listed from various literature study [24- 26], USDA Phytochemical and Ethnobotanical Database [27] and NCBI PubChem Database [28]. The compounds complying with Lipinski's Rule of Five (for drug-likeness properties) and having the ability to penetrate Blood Brain Barrier (BBB), were used for this study. Drug likeness, Human Intestinal Absorption (HIA) property and mutagenicity of these phytochemicals were predicted using the PreADMET server [29]. Online BBB prediction server (version 0.90) equipped with PubChem Fingerprint and AdaBoost algorithm [30] was used in predicting whether a phytochemical is BBB permeable. Molsoft drug-likeness and molecular property prediction server [31] was used to determine the number of hydrogen bond donors (HBD), the number of hydrogen bond acceptors (HBA), the molecular weight of the

ligands and LogP (octanol/water partition coefficient). The details of these properties are listed in Table 3.1.

Table 3.1.: Molecular drug properties of *W. somnifera* phytochemicals selected for inhibition of PARP-1

SN	PubChem CID	Ligands	Lipinski's (Ro5) Criteria				BBB Penetrat-ion	HIA %
			Mol. Wt. (≤500)	HBA (≤10)	HBD (≤5)	LogP (≤5)		
1	443143	Anaferine	224.19	1	2	1.02	BBB+	90.023
2	12306778	Anahygrine	224.19	2	1	1.15	BBB+	94.969
3	222284	Beta-sitosterol	414.39	1	1	9.48	BBB+	100.000
4	124434	Calystegine_B2	175.08	4	5	-2.62	BBB+	36.118
5	1794427	Chlorogenic Acid	354.10	9	6	-0.30	BBB+	20.427
6	441070	Cuscohygrine	224.19	3	0	1.28	BBB+	100.000
7	11850	Dulcitol	182.08	6	6	-3.60	BBB+	12.812
8	92987	Pelletierene	141.12	1	1	0.68	BBB+	94.193
9	14106343	Somniferine	608.25	9	2	3.01	BBB+	95.975
10	5280794	Stigmasterol	412.37	1	1	8.82	BBB+	100.00
11	449293	Tropine	141.12	2	1	0.21	BBB+	99.457
12	54606507	Withacnistin	512.28	7	1	3.63	BBB+	97.473
13	265237	Withaferin A	470.27	6	2	3.21	BBB+	94.740
14	14236711	Withanolide A	454.27	5	1	4.59	BBB-	96.650
15	101559583	Withanolide C	522.24	7	4	2.75	BBB+	88.359
16	21679023	Withanolide G	454.27	5	2	4.94	BBB+	94.478
17	25090669	Withanolide M	468.25	6	2	4.30	BBB+	94.892
18	23266147	Withanolide N	452.26	5	2	5.10	BBB+	94.595
19	23266146	Withanolide O	452.26	5	2	4.78	BBB+	94.592
20	21679034	Withanolide P	454.27	5	2	5.05	BBB+	94.478
21	101281365	Withanolide Q	470.27	6	3	4.08	BBB+	91.644
22	11049407	Withanolide S	504.27	8	5	1.58	BBB+	71.684
23	44566968	Withaphysalin F	484.25	7	2	2.17	BBB+	94.540
24	10096775	Withaphysalin M	482.23	7	1	2.06	BBB+	96.885
25	11752064	Withaphysalin N	484.25	7	1	2.36	BBB+	96.340
26	23266146	Withaphysalin O	512.28	7	1	3.10	BBB+	97.525
27	442877	Withasomnine	184.10	1	0	2.38	BBB+	100.00

Structures for FR257517, PJ34 and Talazoparib (Fig. 3.2.) - potent inhibitors for PARP-1 [32-34] were downloaded in .sdf format from RCSB-Protein Database (PDB) [35]. All the phytochemicals and the inhibitor were converted from .sdf to .pdb format using PyRx-Python prescription 0.8 [36]. The same software was also used for energy minimization of all the ligands by application of mmff94 force field and conjugate gradients optimization algorithm for 200 steps.

3.2.2. Retrieval of PARP-1 Enzyme Structure

The 3-dimensional (3D) structure for PARP-1 was downloaded from RCSB-PDB (PDB ID: 5DS3) [37]. Crystal structure of this enzyme was deposited by Langelier *et al*. as a constitutively active protein structure. The structure consists of 271 amino acids containing the catalytic domain of Human PARP-1 (residues 788-1012). The protein was cloned and expressed in Escherichia coli expression system. Structure determination was performed by X-ray crystallographic method at a resolution of 2.6 Å.

3.2.3. Preparation of Enzyme for Docking

The 3-D structure of PARP-1 was loaded on UCSF Chimera [38] for energy minimization. First, ligands and heteroatoms were removed to clean and optimize the molecule. Heteroatoms present in the PARP-1 structure were polyethylene glycol and sulfate ion. Then energy minimization of the enzyme was performed using steepest descent method for 100 steps (0.02 Å step size) and conjugate gradient method which has ten steps with the step size of 0.02 Å.

3.2.4. Simulating Molecular Docking Studies

Auto Dock Tools 1.5.6 (ADT) [39] was used to perform the docking studies of PARP-1 with FR257517, PJ34 and Talazoparib and *W.somnifera* phytochemicals. The enzyme molecule was assigned Gestgeiger partial charges after merging of nonpolar hydrogen atoms and by applying torsion to the ligands by rotation of all rotatable bonds. Also, the addition of polar hydrogen atoms, application of solvation parameters and Kollman charges were performed using ADT. Among three search algorithm options offered by ADT to analyze active binding with different efficacy, the Lamarckian genetic algorithm (LGA) was utilized for this study. The docking study was performed by creating a grid box near the catalytic domain amino acid residues of

the protein with the number of points 90, 90 and 90, in, Y and Z dimension and values for center of the grid box were assigned as 4.924, 36.5 and 9.798 for X, Y, and Z-center, respectively. Spacing for the grid box was kept at 0.375 Å, and it was ensured that the grid box entirely covers all the active site residues present at the binding site of the enzyme. Space for the translational and rotational walk of the ligands was provided. For docking study of every ligand, 30 independent runs were performed with the maximum number of 27,000 GA operations generated on a single population of 150 individuals. Parameters like the rate of crossover, the rate of gene mutation, and elitism were set to their default values of 0.80, 0.02, and 1, respectively. The second round of molecular docking was performed for high binding affinity phytochemicals by drawing a grid box covering the entire surface of the enzyme to study off-target interactions of the ligands. The grid box was assigned a number of points 116, 126 and 115 in X, Y and Z dimensions, respectively. Offset value was set at -1.025 for X-axis and 4.659 for Y-axis. All the other parameters regarding the docking study were kept similar to that of the first round of docking. For further analysis and visualization of protein-ligand interaction patterns, UCSF Chimera and LigPlot+ (v.1.4.5) [40] softwares were used. This study involved only the lowest energy binding pose of each phytochemical to gain a deeper insight of the hydrogen bonding and hydrophobic interaction patterns manifested by the protein-ligand complexes.

3.3. RESULTS

3.3.1. Analyzing inhibition potential of *W. somnifera* phytochemicals against PARP-1

W. somnifera phytochemicals were docked near the catalytic amino acid residues of PARP-1 for determining the binding parameters. The results obtained for docking studies of all the ligands include lowest binding energy, inhibition constant, hydrogen bonding and hydrophobic

interactions (for 30 docking runs) between the enzyme and the ligands. Comparison of binding energy of the inhibitors and various phytochemicals against PARP-1 is plotted and represented in Fig. 3.3.

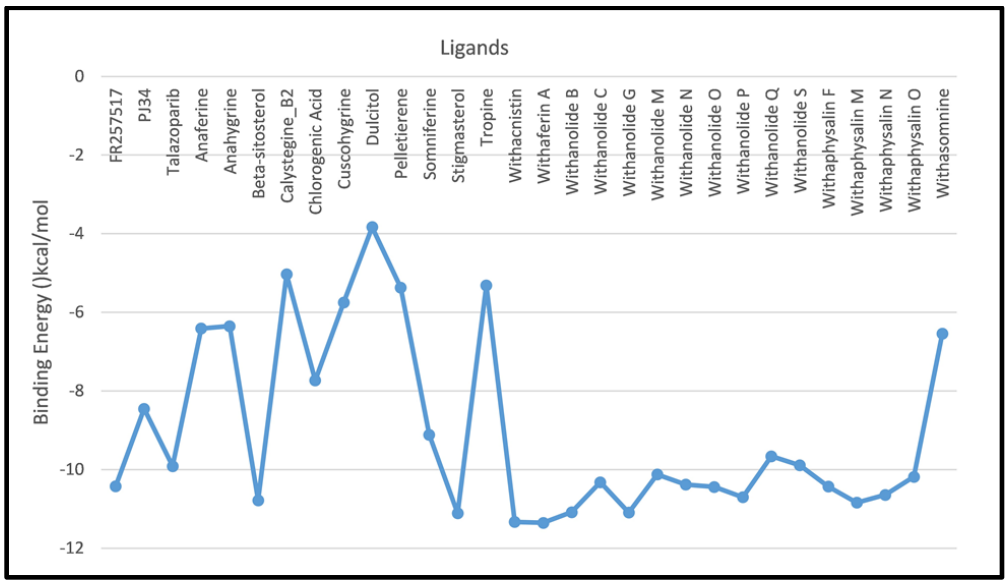

Fig. 3.3.: Comparison of binding energies of inhibitors and *W. somnifera* phytochemicals

The plot for comparison of binding energies summarizes that Withaferin A exhibits lowest binding energy of -11.35 kcal/mol, a value much lower than that of known PARP-1 inhibitors FR257517, PJ34 and Talazoprib which show binding energy values of -10.42 kcal/mol, -8.45 kcal/mol and -9.91 kcal/mol respectively. 11 more compounds including Beta-sitosterol, Stigmasterol, Withacnistin, Withanolide A, Withanolide G, Withanolide O, Withanolide P, Withanolide R, Withaphysalin F, Withaphysalin M and Withaphysalin N bind to PARP-1 with binding energies lower than FR257517, PJ34 and Talazoparib, thus exhibiting higher binding affinity. Though rest of the 15 phytochemicals show elaborate hydrogen bonding with PARP-1, they fail to manifest higher binding affinity towards the protein molecule than the reported inhibitors since the phytochemicals display higher binding energies as compared to the

inhibitors. So, out of the 27 phytochemicals, 12 molecules exhibit lower binding energy as compared to three potent inhibitors of PARP-1, i.e., FR257517, PJ34 and Talazoprib. The details of binding energy, estimated inhibition constant and hydrogen bond formation between the phytochemicals and PARP-1 enzyme are listed in Table-3.2.

Table 3.2.: Detailed Result of Docking Study of PARP-1 and selected Ligands

S. No.	Ligand	PubChem ID	Lowest Binding Energy (kcal/mol)	Estimated Inhibition Constant (K_i)	Amino Acid residues Participating in Hydrogen Bonding with PARP-1 (Residues essential for Hydrogen bond formation with PARP-1 as reported by Kinoshita et al. [24])
	FR257517	--	-10.42	23.06 nM	**Ser 904**, Tyr 896**, Gly 863, Arg 878, Glu 988**
	PJ34	4858	-8.45	637.04 nM	**Gly 863**
	Talazoparib	44819241	-9.91	54.84 nM	**Gly 863**
***Withania somnifera* Phytochemicals**					
1	Anaferine	443143	-6.41	19.97µM	Glu988, Lys 903, Tyr 907, **Gly 863**, His 862, Glu 862, Glu 923, Lys 1000, Asp 965
2	Anahygrine	12306778	-6.35	22.11 µM	Glu988, Tyr 896, **Gly 863**, Glu 809
3	Beta-sitosterol	222284	-10.78	12.57 µM	**Arg 878**, Gly 871, Gly 876, **Glu 988**, Lys 903, Tyr 907
4	Calystegine_B2	124434	-5.03	204.98 µM	Gly 888, Lys 903, **Glu 988**, Met 890, **Gly 863**, **Ser 904**, Tyr 896, Asp 899, Lys 949, Gln 846, Glu 840, Arg 841, Cys 845, Gly 843, Thr 910, Asn 906, Ala 905, Asp 905, Asp 835, Asp 773, Gly 894
5	Chlorogenic Acid	1794427	-7.73	2.17 µM	Tyr 896, Gly 894, **Ser 904**, **Gly 863**, **Arg 878**, Gly 888, Tyr 889, Ala 880, Arg 865, Tyr 907, Ser 907, Ser 864, **Glu 988**, His 862, Met 890, Asn 868
6	Cuscohygrine	441070	-5.75	61.28 µM	Tyr 896, **Gly 863**, Lys 903
7	Dulcitol	11850	-3.83	1.55 µM	Tyr 889, **Arg 878**, Tyr 896, Gly 894, Ala 880, Gly 894, Asn 868, Lys 903, Gly 876, Asn 906, Thr 910, Ser 864, Arg 865, Gly 888, Met 890, Leu 941, Lys 940, Tyr 907, Leu 985
8	Pelletierene	92987	-5.37	115.8 µM	Tyr 896, Lys 1000
9	Somniferine	14106343	-9.11	211.22 nM	**Arg 878**, His 862

10	Stigmasterol	5280794	-11.11	7.17 nM	Gly 871, **Arg 878**, **Glu 988**, Gly 876, Tyr 907
11	Tropine	449293	-5.31	129.13 µM	**Ser 904**, **Gly 863**, Ala 905, Thr 910, Tyr 896, His 862
12	Withacnistin	54606507	-11.33	4.94 nM	His 862, **Arg 878**, Tyr 894, **Gly 863**, Ala 880
13	Withaferin A	265237	-11.35	4.79 nM	**Arg 878**, Tyr 896, Met 890, **Ser904**, **Gly 863**, His 862, Gly 876
14	Withanolide A	14236711	-11.08	7.54 nM	**Arg 878**, **Gly 863**, Tyr 896, Tyr 907, His 862
15	Withanolide C	101559583	-10.32	27.04 nM	Tyr 889, Gly 888, Tyr 907, His 862, Tyr 896, **Gly 863**, **Arg 878**, Gly 894, Asn 868
16	Withanolide G	21679023	-11.09	7.37 nM	**Gly 863**, His 862, **Arg 878**, Ser 864, Met 890
17	Withanolide M	25090669	-10.12	38.02 nM	His 862, **Arg 878**, **Gly 863**, Gly 894
18	Withanolide N	23266147	-10.38	41.63 nM	Tyr 896, Gly 894, **Gly 863,** Met 890, Gly 888, Gly 876, **Arg 878**, **Ser 904**
19	Withanolide O	23266146	-10.44	22.27 nM	Gly 894, Tyr 896, **Arg 878**, **Gly 863**, Met 890, Gly 888
20	Withanolide P	21679034	-10.70	14.41 nM	Gly 894, Tyr 896
21	Withanolide Q	101281365	-9.66	83.57 nM	**Arg 878**, Gly 876, Gly 888, **Gly 863**, His 862, Ser 864, Asn 868, Met 890, Gly 894, Tyr 907
22	Withanolide S	11049407	-9.89	56.77 nM	**Arg 878**, Tyr 896, Gly 894, **Gly 863**, Ser 864, Met 890, Gly 888
23	Withaphysalin F	44566968	-10.43	22.46 nM	Ser 864, His 862
24	Withaphysalin M	10096775	-10.84	11.26 nM	**Arg 878**, His 862
25	Withaphysalin N	11752064	-10.64	15.92 nM	His 862, **Arg 878**, **Gly 863**
26	Withaphysalin O	23266146	-10.18	34.63 nM	His 862, **Gly 863**, Tyr 896, Met 890, **Arg 878**
27	Withasomnine	442877	-6.54	16.18 µM	**Gly 863**

3.3.2. Analysis of Binding Mechanism of Inhibitors with PARP-1

Among the 12 compounds demonstrating higher binding affinity towards PARP-1, five phytochemicals showing binding energy lower than -11.00 kcal/mol were regarded as highly potent inhibitors of PARP-1 and were further analyzed for visualizing their binding characteristics using LigPlot+ (v.1.4.5). Interaction pattern of these five molecules namely Withaferin A, Withacnistin, Stigmasterol, Withanolide A and Withanolide G were compared with that of FR257517 (binding energy: -10.42 kcal/mol), PJ34 (binding energy: -8.45 kcal/mol) and Talazoparib (binding energy: -9.91 kcal/mol). FR257517 interacts with the

Arg878 residue of PARP-1 with two hydrogen bonds formed between its fluorophenyl group and two nitrogen atoms present in the polar side chain of the amino acid with bond lengths of 2.73 and 2.76 Å (Fig. 3.4.a). It shows a hydrogen bonding between a nitrogen atom of the amino acid Glycine 863 and an oxygen atom with the bond length of 2.77 Å (Fig. 3.4.a). FR257517 also shows hydrophobic interaction with various amino acid residues namely Glu 988, Tyr 896, Phe 897, His 862, Ser 904, Gly 876, Leu 877, Gly 894, Ile 895, Lys 903 and Ala 898 (Fig. 3.4.a). The inhibitors PJ34 and Talazoparib each form two hydrogen bonds with oxygen and nitrogen atoms of Gly863 residue. Bond lengths for interaction between PJ34 and Gly 863 are 3.11 Å (for N atom) and 2.69 Å (for O atom) and those for Talazoparib and Gly 863 interaction are 2.70 Å (for N atom) and 2.84 Å (for O atom) (Fig. 3.4.b, 3.4.c). PJ34 hydrophobically interacts with Gly 894, Tyr 889, Ala 898, Tyr 907, His 862, Ser 904, Phe 897, Lys 903, Glu 988, Tyr 896 and Ile 895, whereas Talazoparib exerts hydrophobic interactions with Ser904, Tyr 907, Glu988, Gly888, Ala898, Met 890, Tyr 896, His862, Lys903 and Phe 897 (Fig. 3.4.b, 3.4.c). Withaferin A, the phytochemical exhibiting lowest binding energy forms 6 hydrogen bonds with Gly 888, Met 890, Tyr 896, Arg 878 and Gly 876 and hydrophobic interactions with Gly 871, Ile 872, His 862, Leu 877, Gly 894, Tyr 889, Tyr 907, Ala 880 and Gln 875 (Fig 3.5.a). Withacnistin, which shows binding energy quite closer to Withaferin A, forms hydrogen bonds with Arg 878, Ser 864, His 862 and Tyr 896 and hydrophobically interacts with, Leu 877, Gly 894, Ile 895, Ser 904, Phe 897, Gly 863, Trp 862, Ile872 and Tyr 907 (Fig 3.5.b). Stigmasterol shows hydrogen bond formation with Arg 878 and Gly 871 and hydrophobically interacts with residues similar to those of FR257517 except Gly 894 and Ile 895 (Fig 3.5.c). Other amino acid residues of PARP-1 exhibiting hydrophobic interactions with Stigmasterol are Trp861, Asn 868, Tyr 907, Ile 872, Gln 875 and Ser 864.

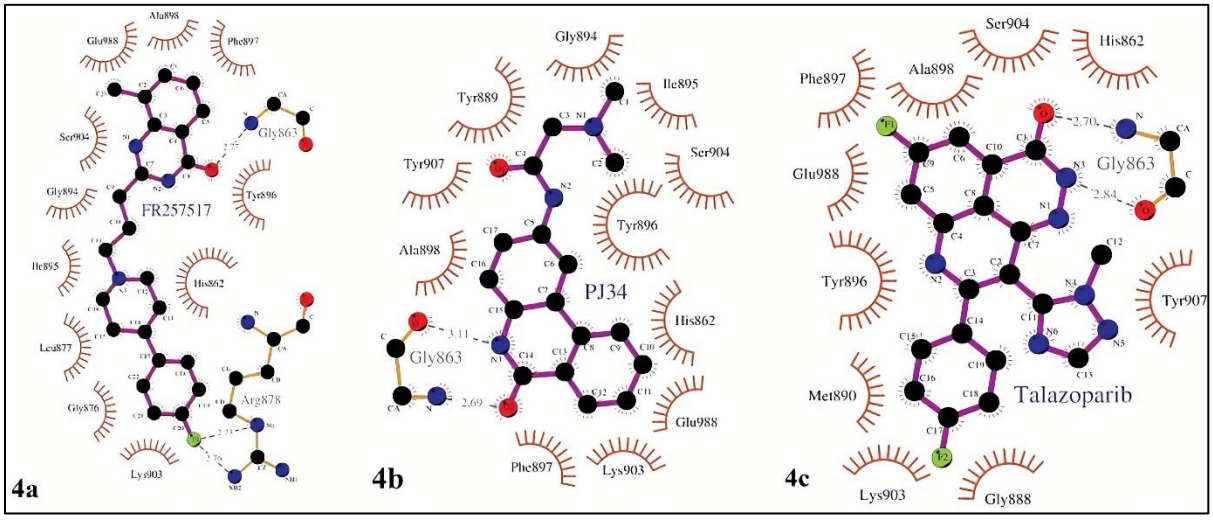

Fig. 3.4.a-c: Interaction pattern of inhibitors FR257517, PJ34 and Talazoparib with amino acid residues of catalytic domain of PARP-1

Ligand bond

Non-ligand bond

2.39 Hydrogen bond and its length

Leu135(A) Non-ligand residues involved in hydrophobic contact(s)

Corresponding atoms involved in hydrophobic contact(s)

Among these five Withanolides, Stigmasterol shows the highest number (16) of hydrophobic interactions, which is also greater than all three reported inhibitors. Withanolide G forms three hydrogen bonds with Gly 863, Arg 878 and His 862 whereas Withanolide A forms two hydrogen bonds with residues Gly 863 and Arg 878. These two withanolides also show extensive hydrophobic interactions with various amino acid residues (Fig 3.5.d, 3.5.e). All of these five phytochemicals display lower binding energy while interacting with PARP-1 in comparison to reported inhibitors.

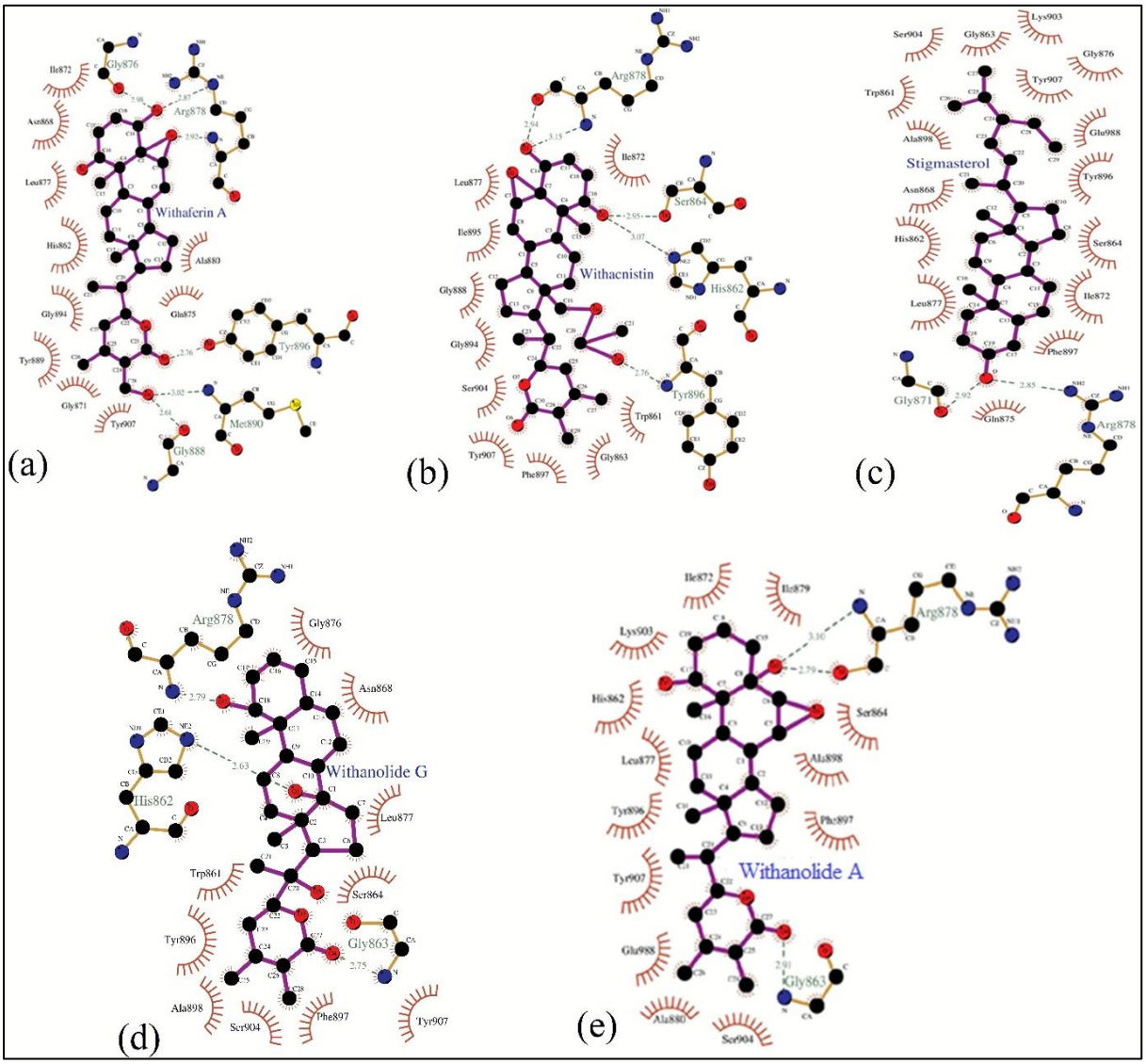

Fig. 3.5.a-e: Interaction pattern of *W.somnifera* phytochemicals having binding energy lower than -11.00 kcal/mol with PARP-1 catalytic domain

3.3.3. Analysis of off-target interaction of the high-affinity phytochemicals

Among the five phytochemicals with a high binding affinity towards PARP-1, three phytochemicals exhibit a low-affinity interaction at sites other than the designated catalytic sites of the enzyme. Stigmasterol and Withacnistin, each reveals a single off-target interaction

pose with a binding energy of -8.25 kcal/mol and -6.53 kcal/mol respectively. Withaferin A, however, shows two off-target binding poses, but with low binding affinities (binding energy: -7.72 kcal/mol and -6.29 kcal/mol). Withanolide A and Withanolide G along with all the known inhibitors (except FR257517) do not manifest any off-target binding affinities. The details regarding binding energy, inhibition constant and involved residues for off-target binding of the ligands are listed in Table 3.3., and the binding poses for off-target and active site interactions for the ligands are illustrated in Fig. 3.6-3.8.

Table 3.3.: Details of off-target interaction between five high affinity phytochemicals and PARP-1

Serial No	Ligand	Binding Energy Manifested In Off-Target Binding Pose (kcal/mol)	Estimated Inhibition Constant (K_i)	Amino Acid residues Participating in Hydrogen Bonding with PARP-1 (outside the catalytic site)
	FR257517	-4.9		Ser 911
	PJ34	--	--	--
	Talazoparib	--	--	--
***Withania somnifera* Phytochemicals**				
1	Stigmasterol	-8.25	897.73 nM	Lys 893
2	Witachcnistin	-6.53	16.47 µM	Ser 911, Lys 1010
3	Withaferin A	-6.29	8.43 µM	Thr 867
		-7.72	2.18 µM	Lys 796
4	Withanolide B	--	--	--
5	Withanolide G	--	--	--

In the case of the ligands manifesting off-target interaction, affinity towards the site other than the catalytic domain is much lower than their affinity towards the active site of PARP-1.

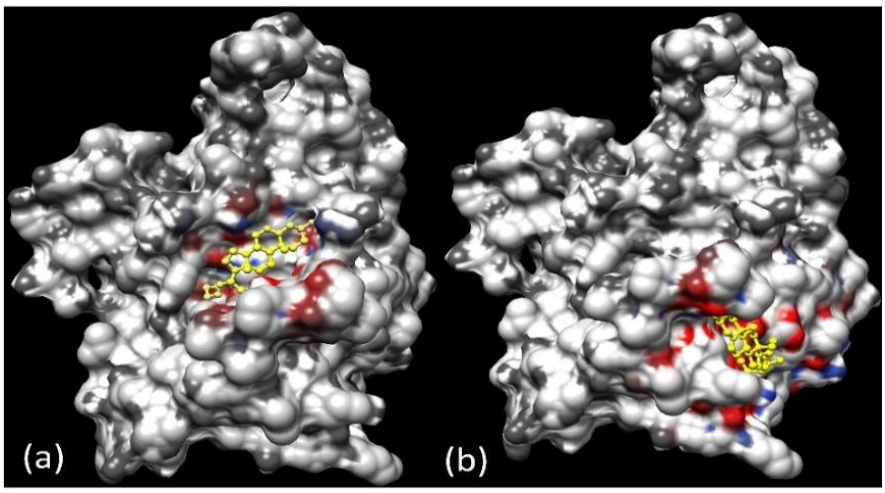

Fig. 3.6.: Stigmasterol binding at (a) the catalytic site; (b) off-target domain.

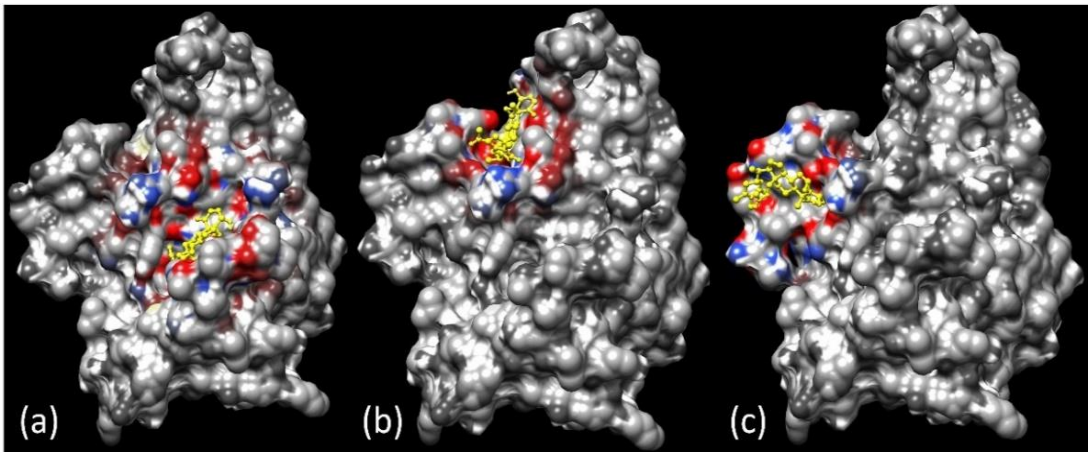

Fig. 3.7.: Withaferin A binding at (a) the catalytic site; (b, c) off-target domains.

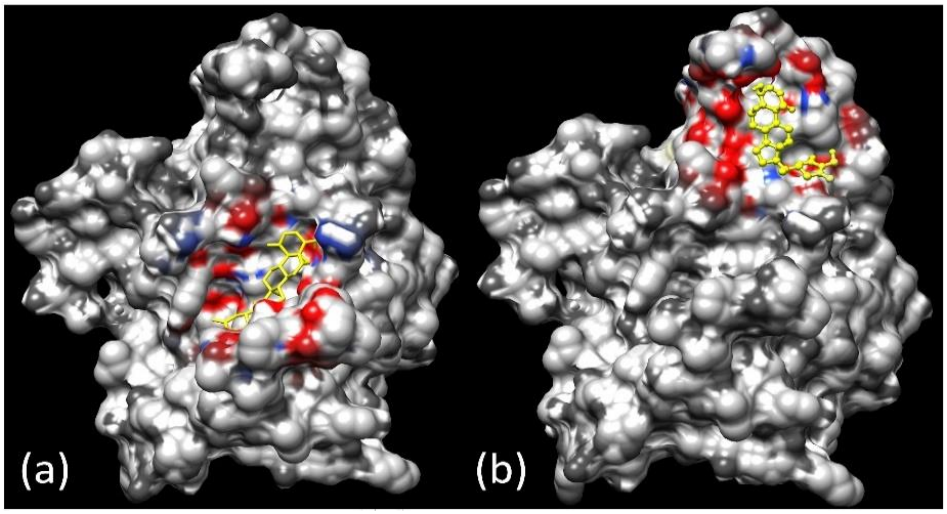

Fig. 3.8.: Withacnistin binding at (a) the catalytic site; (b) off-target domain.

3. 4. DISCUSSION

Overproduction of nitric oxide (NO) due to nNOS activation in an ROS enriched environment leads to the generation of peroxynitrite [41,42], which is a potent oxidant playing a highly important role in neurotoxicity [43,44]. Peroxynitrite production results in DNA damage and thereby triggers activation of PARP-1, an enzyme involved in DNA repair, DNA replication, gene expression, and regulation, finally causing cell death via depletion of cellular energy, a phenomenon which researchers have tried to explain by "suicide hypotheses" proposed by Berger et al. [5-6]. Though the actual mechanism of PARP-1 mediated cell death is not yet understood completely, inhibition or genetic knockout of PARP-1 has ameliorated neurodegenerative conditions establishing PARP-1 as a potent therapeutic target for combating neurotoxicity [45-47]. PARP-1 is a 113 kDa protein possessing a large active site which can be classified as the acceptor site and the donor site [48]. Standard PARP1 inhibitors are known to bind the nicotinamide ribose binding site, or NI site [32, 49]. Previous *in-silico* study of the catalytic domain of PARP-1 has revealed that hydrogen bond formation between residues Gly 863, Arg 878 and Ser 904 and the ligand is necessary for binding pocket stability [49, 50]. Specifically, the residues Gly 863 and Ser 904 are reported to be primarily responsible for the establishment of inhibitory capacity of the PARP-1 inhibitors [49]. Most synthetic PARP-1 inhibitors compete with NAD+ to bind the catalytic domain and tend to block different enzymatic pathways which involve NAD+ [51]. Also, high toxicity and other side effects associated with synthetic PARP-1 inhibitors necessitate the development of novel PARP-1 inhibitors [51]. So, this study attempted to evaluate the effectiveness of phytochemicals of *Withania somnifera*, an Indian herb commonly known as *Ashwagandha*, in inhibiting PARP-1 activity. *Withania somnifera* or *Ashwagandha* is conventionally used as nerve tonic [52],

memory and cognition enhancer [53-54] and also as therapy of neurodegenerative disorders including cerebral ischemia [55-56]. A recent scientific study has reported that root extract of *W. somnifera* successfully combats ischemic pathophysiology by impairing the PARP1-AIF pathway [57]. We have selected 27 phytochemicals of *Ashwagandha* including the Withanolides, which reportedly contribute to neuroprotective potential of the herb for the study. Though the phytochemicals might show a synergestic effect when the plant extract is administered, it may or may not be very effective. It is reported that the bioactive compounds present in plant extracts might be agonists or antagonists of the neurotransmitters [58]. Understanding the mechanism of the constituent phytochemicals, might help in identifying suitable candidates for designing of future neurotherapeutic drugs. Since the extract of *W. somnifera* is reported to interfere with the PARP1-AIF pathway, studying the ability of its constituent phytochemicals in inhibiting the enzyme PARP1 can reveal potent molecules for drug development.

In the present study, 12 constituent phytochemicals of *W. somnifera* showed higher inhibition potential than the reported inhibitor FR257517, PJ34 and even Talazoparib, which is currently in Phase-III clinical trial [19]. Among these 12 inhibitors, 5 compounds reveal exceptionally high inhibiting capacity with binding energy lower than -11.00 (binding energy of FR257517, PJ34 and Talazoparib being -10.42 kcal/mol, -8.45 kcal/mol and -9.91 kcal/mol respectively). Withaferin A shows highest binding affinity as it shows the lowest binding energy of -11.35kcal/mol and further analysis of PARP1-Withaferin A complex using LigPlot+ reveals that similar to FR257517 it forms two hydrogen bonds with amino acid residue Arg 878. This is an important aspect of interaction pattern of Withaferin A with PARP-1 since the interaction between carbonyl oxygen of the ligand and the residue Arg 878 is required for stabilization of

the PARP1-ligand complex [49]. Withaferin A also exhibits hydrogen bonding with amino acid residues Met 890, Ser 904, His 862 and Gly 876 (Fig. 3.5.a), but does not interact with Gly 863 (FR257517, PJ34 and Talazoparib interact with Gly 863 residue), which is required for improving interaction between ligand and PARP-1 [49,51]. Among various hydrophobic interactions exhibited by it, this phytochemical notably interacts with His 862, Tyr 907, Ala 880 and Ile 872, which reportedly constitute the ligand-binding site of PARP-1 [49]. Among the rest of four phytochemicals exhibiting binding energy less than -11 kcal/mol, Withanolide A and Withanolide G show almost similar binding energy (-11.08kcal/mol and -11.09 kcal/mol respectively) and are the only two phytochemicals to form hydrogen bond with the Gly 863 residue (Fig 3.5.d-3.5.e), which is reported to have 52% hydrogen bond occupancy among the key amino acids, Arg 878 residue being the second abundant one (40% of hydrogen bond occupancy) [49]. Both the phytochemicals form hydrogen bonds with Arg 878 residue, which performs a critical role to stabilize adenosine part of NAD+ (substrate for PARP1) [59]. The ligands hydrophobically interact with residues like Ser 904, which has 33% bond occupancy among the key amino acids present in the active site of PARP-1 [49], Tyr 907 and Ser 864, both of which are prominently present in the ligand binding site of PARP-1 [49]. His 862 and Glu 988 are two more residues which significantly contribute to the interactions taking place in the active site [60, 61]. In this study also, we have found that while Withanolide G forms a hydrogen bond with His 862, Withanolide A hydrophobically interacts with the same, which is a mechanism similar to that of all three reported inhibitors FR257517, PJ34 and Talazoparib. Withanolide A also hydrophobically interacts with Glu 988, the residue responsible for NAD+ catalysis activity of PARP-1 [62, 63] and Lys 903, which is necessary for DNA polymerization [64] but Withanolide G does not show any interaction with these two residues. However, FR257517, PJ34 and Talazoparib exhibit interaction with Glu 988 and Lys 903. The other two

molecules Withacnistin and Stigmasterol (binding energy -11.33 kcal/mol and -11.11 kcal/mol respectively) form hydrogen bonds with Arg 878 residue, similar to inhibitor FR257517, but unlike the three reported inhibitors, these two phytochemicals show no hydrogen bonding with the critical residue Gly 863, but forms hydrophobic interaction with the residue. Withacnistin forms hydrogen bond with His 862, presence of which is required for binding interactions at the active site [60], and Ser 864, a highly significant residue present in the ligand binding site of PARP-1 [49], but Stigmasterol hydrophobically interacts with both of these residues. Among the other important residues present at the ligand binding site of PARP-1, Stigmasterol hydrophobically interacts with Glu 988 (required for catalysis of NAD^+) [62, 63], Ser 864 and Ser 904 (constituent residues of ligand binding site of PARP-1), whereas Withacnistin shows no interaction with Glu 988 but forms hydrogen bond with Ser 864 and hydrophobically interacts with Ser 904. Withacnistin also shows hydrogen bonding with His 862, another significant residue present at the active site [60].

Whether a ligand possesses higher affinity towards a site other than the active site of the target protein, is a matter of importance in inhibitor screening. The Higher affinity of a ligand towards an off-target site may lead to side-effects [65]. In this study, the off-target interaction of the five high-affinity phytochemicals reveals lower or no binding affinity of the ligands towards sites other than the active site of the enzyme. Stigmasterol, Withacnistin and Withaferin A displayed off-target interaction, but the binding energies for all three ligands were significantly higher compared to their binding energy in catalytic site interaction. Withanolide G and Withanolide A display no off-target interaction. It can be inferred from such binding characteristics that these phytochemicals are prone to bind to the catalytic domain of the enzyme.

These five phytochemicals of *W. somnifera* can be regarded as potent PARP-1 inhibitors, because not only they exhibit higher binding affinity towards the enzyme as compared to reported inhibitors FR25517, PJ34 and Talazoparib, they also show greater number of hydrogen bond formation and hydrophobic interaction with most of the crucial residues of the active site which are responsible for inhibition of the enzyme. The phytochemicals also have much lower inhibition constant (Ki) values than all the three reported inhibitors. As compared to the binding pattern of Talazoparib (already in Phase-III clinical trial), Withanolide A shows almost similar interaction pattern regarding hydrogen bond formation and hydrophobic interactions (Fig. 3.9).

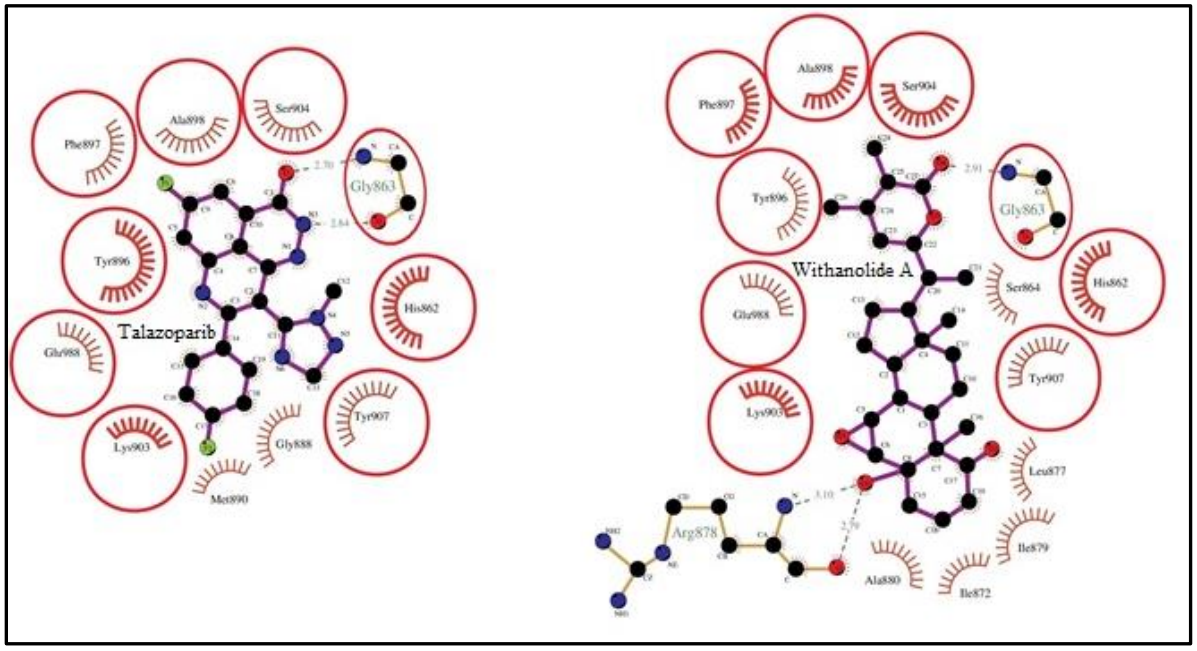

Fig. 3.9.: Comparison of hydrogen binding and hydrophobic interaction pattern of Talazoparib and Withanolide A with PARP-1 catalytic domain.

Further, it also interacts hydrophobically with Ile 879, Ala 880 and Ile 872, residues previously reported as crucial residues for binding of ligands and also forms a hydrogen bond with Arg

878 (one of the key amino-acids to form hydrogen bonds in the enzyme-inhibitor complex) [48]. The phytochemical also has no off-target affinity and only binds the catalytic domain of the enzyme with high binding affinity. In terms of binding energy, Withaferin A can be considered as the most potent inhibitor, but taking into account the criteria of binding energy, hydrogen bonds and hydrophobic interactions, Withanolide A can surely be a worthy candidate for PARP-1 inhibition.

3. 5. CONCLUSION

This *in-silico* study involves 27 WS phytochemicals which are screened for their ability to inhibit PARP-1, an important mediator of caspase-independent cell death pathway involved in neurotoxicity. Here, we report 12 phytochemicals of *W. somnifera* showing a higher affinity towards PARP-1 as compared to inhibitors FR257517, PJ 34 and Talazoparib. Amongst these 12 inhibitors, 5 compounds, Withaferin A, Withacnistin, Stigmasterol, Withanolide G and Withanolide A, show a remarkably high binding affinity (binding energy < -11.00 kcal/mol) towards PARP-1 and forms a higher number of hydrogen bonds and hydrophobic interactions as compared to these three inhibitors. Withaferin A binds to the catalytic site of the enzyme with the highest affinity since it shows lowest binding energy among all the phytochemicals analyzed and Withanolide A, besides showing low binding energy, also exhibits an almost exact pattern of hydrogen bonding and hydrophobic interactions as that of Talazoparib. It has been previously reported that inhibition of PARP-1 leads to subsequent reversal of cell death and the PARP-1 inhibition strategy can be exploited to combat neurotoxic conditions. Our study establishes the potential of five WS phytochemicals as novel inhibitors of PARP-1.

References:

[1] Hong, S. J., Dawson, T. M., & Dawson, V. L. (2004). Nuclear and mitochondrial conversations in cell death: PARP-1 and AIF signaling. Trends in pharmacological sciences, 25(5), 259-264.

[2] Yu, S. W., Wang, H., Dawson, T. M., & Dawson, V. L. (2003). Poly (ADP-ribose) polymerase-1 and apoptosis inducing factor in neurotoxicity. Neurobiology of disease, 14(3), 303-317.

[3] Virág, L., & Szabó, C. (2002). The therapeutic potential of poly (ADP-ribose) polymerase inhibitors. Pharmacological reviews, 54(3), 375-429.

[4] Ha, H. C., & Snyder, S. H. (2000). Poly (ADP-ribose) polymerase-1 in the nervous system. Neurobiology of disease, 7(4), 225-239.

[5] Berger, S. J., Sudar, D. C., & Berger, N. A. (1986). Metabolic consequences of DNA damage: DNA damage induces alterations in glucose metabolism by activation of poly (ADP-ribose) polymerase. Biochemical and biophysical research communications, 134(1), 227-232.

[6] Berger, N. A., Sims, J. L., Catino, D. M., & Berger, S. J. (1983). Poly (ADP-ribose) polymerase mediates the suicide response to massive DNA damage: studies in normal and DNA-repair defective cells. Proceedings of the International Symposia of the Princess Takamatsu Cancer Research Fund, 13, 219-226.

[7] Du, L., Zhang, X., Han, Y. Y., Burke, N. A., Kochanek, P. M., Watkins, S. C., et al. (2003). Intra-mitochondrial poly (ADP-ribosylation) contributes to NAD+ depletion and cell death induced by oxidative stress. Journal of Biological Chemistry, 278(20), 18426-18433.

[8] Vosler, P. S., Sun, D., Wang, S., Gao, Y., Kintner, D. B., Signore, A. P., et al. (2009). Calcium dysregulation induces apoptosis-inducing factor release: cross-talk between PARP-1- and calpain-signaling pathways. Experimental neurology, 218(2), 213-220.

[9] Li, X., Klaus, J. A., Zhang, J., Xu, Z., Kibler, K. K., Andrabi, S. A., et al. (2010). Contributions of poly (ADP- ribose) polymerase- 1 and -2 to nuclear translocation of apoptosis- inducing factor and injury from focal cerebral ischemia. Journal of neurochemistry, 113(4), 1012-1022.

[10] Susin, S. A., Lorenzo, H. K., Zamzami, N., Marzo, I., Snow, B. E., Brothers, G. M., et al. (1999). Molecular characterization of mitochondrial apoptosis-inducing factor. Nature, 397(6718), 441-446.

[11] Yu, S. W., Wang, H., Poitras, M. F., Coombs, C., Bowers, W. J., Federoff, H. J., et al. (2002). Mediation of poly (ADP-ribose) polymerase-1-dependent cell death by apoptosis-inducing factor. Science, 297(5579), 259-263.

[12] Cregan, S. P., Fortin, A., MacLaurin, J. G., Callaghan, S. M., Cecconi, F., Yu, S. W., et al. (2002). Apoptosis-inducing factor is involved in the regulation of caspase-independent neuronal cell death. J Cell Biol, 158(3), 507-517.

[13] Dawson, V. L., & Dawson, T. M. (2004). Deadly conversations: nuclear-mitochondrial cross-talk. Journal of bioenergetics and biomembranes, 36(4), 287-294.

[14] Eliasson, M. J., Sampei, K., Mandir, A. S., Hurn, P. D., Traystman, R. J., Bao, J., et al. (1997). Poly (ADP-ribose) polymerase gene disruption renders mice resistant to cerebral ischemia. Nature medicine, 3(10), 1089-1095.
[15] Szabó, C., & Dawson, V. L. (1998). Role of poly (ADP-ribose) synthetase in inflammation and ischaemia–reperfusion. Trends in Pharmacological Sciences, 19(7), 287-298.
[16] Martire, S., Fuso, A., Mosca, L., Forte, E., Correani, V., Fontana, M, et al. (2016). Bioenergetic Impairment in Animal and Cellular Models of Alzheimer's Disease: PARP-1 Inhibition Rescues Metabolic Dysfunctions. Journal of Alzheimer's Disease, 54(1), 307-324.
[17] Outeiro, T. F., Grammatopoulos, T. N., Altmann, S., Amore, A., Standaert, D. G., Hyman, B. T., & Kazantsev, A. G. (2007). Pharmacological inhibition of PARP-1 reduces α-synuclein-and MPP+-induced cytotoxicity in Parkinson's disease in vitro models. Biochemical and biophysical research communications, 357(3), 596-602.
[18] De Bono JS, Mina LA, Gonzalez M, Curtin NJ, Wang E, Henshaw JW, et al. (2013). First-in-human trial of novel oral PARP inhibitor BMN 673 in patients with solid tumors. J Clin Oncol, 31:(suppl; abstr), 2580-2580.
[19] Smith, M. A., Reynolds, C. P., Kang, M. H., Kolb, E. A., Gorlick, R., Carol, et al. (2015). Synergistic activity of PARP inhibition by talazoparib (BMN 673) with temozolomide in pediatric cancer models in the pediatric preclinical testing program. Clinical Cancer Research, 21(4), 819-832.
[20] Murai J, Huang SY, Das BB, Renaud A, Zhang Y, Doroshow JH, et al. (2012). Trapping of PARP1 and PARP2 by clinical PARP inhibitors. Cancer Res;72:5588–99.
[21] Sankar, S., Manivasagam, T., Krishnamurti, A., & Ramanathan, M. (2007). The neuroprotective effect of Withania somnifera root extract in MPTP-intoxicated mice: An analysis of behavioral and biochemical varibles. Cellular and molecular biology letters, 12(4), 473-481.
[22] Ahmad, M., Saleem, S., Ahmad, A. S., Ansari, M. A., Yousuf, S., Hoda, M. N., & Islam, F. (2005). Neuroprotective effects of Withania somnifera on 6-hydroxydopamine induced Parkinsonism in rats. Human & experimental toxicology, 24(3), 137-147.
[23] Jain, S., Shukla, S. D., Sharma, K., & Bhatnagar, M. (2001). Neuroprotective Effects of Withania somnifera Dunn. in Hippocampal Sub- regions of Female Albino Rat. Phytotherapy research, 15(6), 544-548.
[24] Kumar, P., & Kumar, A. (2009). Possible neuroprotective effect of Withania somnifera root extract against 3-nitropropionic acid-induced behavioral, biochemical, and mitochondrial dysfunction in an animal model of Huntington's disease. Journal of medicinal food, 12(3), 591-600.
[25] Kumar, G., & Patnaik, R. (2016). Exploring neuroprotective potential of Withania somnifera phytochemicals by inhibition of GluN2B-containing NMDA receptors: An in silico study. Medical hypotheses, 92, 35-43.
[26] Kumar, G, Paliwal P., & Patnaik R. (2017). Withania somnifera Phytochemicals Confer Neuroprotection by Inhibition of the Catalytic Domain of Human Matrix Metalloproteinase-9. Letters in Drug Design & Discovery, 14, 1-10.DOI: 10.2174/1570180814666161121111811

[27] Search Phytochemical Databases. leffingwell.com/plants.htm (Accessed December 12, 2016)
[28] Chemical Structures. National Center for Biotechnology Information.ncbi.nlm.nih.gov/pccompound (Accessed December 19, 2016)
[29] Lee, S. Lee, I. Kim, H. Chang, G. Chung, J. No, K. (2002). The PreADME Approach: Web-based program for rapid prediction of physico-chemical, drug absorption and drug-like properties. EuroQSAR 2002 Designing Drugs and Crop Protectants: Processes, Problems and Solutions 2003, 418-420.
[30] Blood-Brain Barrier Predictor. cbligand.org/BBB/predictor.php. (Accessed January 5, 2017)
[31] Drug-Likeness and Molecular Property Prediction. Molsoft L.L.C.molsoft.com/mprop/ (Accessed December 22, 2016).
[32] Kinoshita, T., Nakanishi, I., Warizaya, M., Iwashita, A., Kido, Y., Hattori, K., & Fujii, T. (2004). Inhibitor- induced structural change of the active site of human poly (ADP- ribose) polymerase. FEBS letters, 556(1-3), 43-46.
[33] Huang SH, Xiong M, Chen XP, Xiao ZY, Zhao YF, Huang ZY., (2008) PJ34, an inhibitor of PARP-1, suppresses cell growth and enhances the suppressive effects of cisplatin in liver cancer cells. Oncol Rep, 20(3):567-72.
[34] G E Konecny and R S Kristeleit. (2016). PARP inhibitors for BRCA1/2-mutated and sporadic ovarian cancer: current practice and future directions. Br. J. Cancer, 115, 1157–1173.
[35] Berman, H. M., Westbrook, J., Feng, Z., Gilliland, G., Bhat, T. N., Weissig, H., et al. (2000). The protein data bank. Nucleic acids research, 28(1), 235-242.
[36] Dallakyan, S., & Olson, A. J. (2015). Small-molecule library screening by docking with PyRx. Chemical Biology: Methods and Protocols, 1263, 243-250.
[37] Dawicki-McKenna, J. M., Langelier, M. F., DeNizio, J. E., Riccio, A. A., Cao, C. D., Karch, K. R., et al. (2015). PARP-1 activation requires local unfolding of an autoinhibitory domain. Molecular cell, 60(5), 755-768.
[38] Pettersen, E. F., Goddard, T. D., Huang, C. C., Couch, G. S., Greenblatt, D. M., Meng, E. C., & Ferrin, T. E. (2004). UCSF Chimera—a visualization system for exploratory research and analysis. Journal of computational chemistry, 25(13), 1605-1612.
[39] Sanner, M. F. (1999). Python: a programming language for software integration and development. J Mol Graph Model, 17(1), 57-61.
[40] Laskowski, R. A., & Swindells, M. B. (2011). LigPlot+: multiple ligand–protein interaction diagrams for drug discovery, 51 (10), 2778–2786.
[41] Beckman, J. S. (1991). The double-edged role of nitric oxide in brain function and superoxide-mediated injury. Journal of developmental physiology, 15(1), 53-59.
[42] Beckman, J. S., & Crow, J. P. (1993). Pathological implications of nitric oxide, superoxide and peroxynitrite formation. Biochemical Society Transactions, 21 (2) 330-334.
[43] Zhang, Y., Wang, H., Li, J., Jimenez, D. A., Levitan, E. S., Aizenman, E., & Rosenberg, P. A. (2004). Peroxynitrite-induced neuronal apoptosis is mediated by intracellular zinc release and 12-lipoxygenase activation. Journal of Neuroscience, 24(47), 10616-10627.

44] Xie, Z., Wei, M., Morgan, T. E., Fabrizio, P., Han, D., Finch, C. E., & Longo, V. D. (2002). Peroxynitrite mediates neurotoxicity of amyloid β-peptide1–42-and lipopolysaccharide-activated microglia. Journal of Neuroscience, 22(9), 3484-3492.
[45] Tanaka, Y., Yoshihara, K., Tohno, Y., Kojima, K., Kameoka, M., & Kamiya, T. (1995). Inhibition and down-regulation of poly (ADP-ribose) polymerase results in a marked resistance of HL-60 cells to various apoptosis-inducers. Cellular and molecular biology (Noisy-le-Grand, France), 41(6), 771-781.
[46] Hagberg, H., Wilson, M. A., Matsushita, H., Zhu, C., Lange, M., Gustavsson, M., et al. (2004). PARP- 1 gene disruption in mice preferentially protects males from perinatal brain injury. Journal of neurochemistry, 90(5), 1068-1075.
[47] Sahaboglu, A., Tanimoto, N., Kaur, J., Sancho-Pelluz, J., Huber, G., Fahl, E., et al. (2010). PARP1 gene knock-out increases resistance to retinal degeneration without affecting retinal function. PloS one, 5(11), e15495.
[48] Ruf, A., Rolli, V., de Murcia, G., & Schulz, G. E. (1998). The mechanism of the elongation and branching reaction of poly (ADP-ribose) polymerase as derived from crystal structures and mutagenesis. Journal of molecular biology, 278(1), 57-65.
[49] Salmas, R. E., Unlu, A., Yurtsever, M., Noskov, S. Y., & Durdagi, S. (2016). In silico investigation of PARP-1 catalytic domains in holo and apo states for the design of high-affinity PARP-1 inhibitors. Journal of enzyme inhibition and medicinal chemistry, 31(1), 112-120.
[50] Ruf, A., de Murcia, G., & Schulz, G. E. (1998). Inhibitor and NAD+ Binding to Poly (ADP-ribose) Polymerase As Derived from Crystal Structures and Homology Modeling†. Biochemistry, 37(11), 3893-3900.
[51] Malyuchenko, N. V., Kulaeva, O., Kirpichnikov, M., & Studitskiy, V. (2015). PARP1 inhibitors: Antitumor drug design. Acta Naturae (англоязычная версия), 7(3 (26)).
[52] Kulkarni, S. K., & Dhir, A. (2008). Withania somnifera: an Indian ginseng. Progress in neuro-psychopharmacology and biological psychiatry, 32(5), 1093-1105.
[53] Bhattacharya, S. K., Kumar, A., & Ghosal, S. (1995). Effects of glycowithanolides from Withania somnifera on an animal model of Alzheimer's disease and perturbed central cholinergic markers of cognition in rats. Phytotherapy Research, 9(2), 110-113.
[54] Sehgal, N., Gupta, A., Valli, R. K., Joshi, S. D., Mills, J. T., Hamel, E., et al. (2012). Withania somnifera reverses Alzheimer's disease pathology by enhancing low-density lipoprotein receptor-related protein in liver. Proceedings of the National Academy of Sciences, 109(9), 3510-3515.
[55] RajaSankar, S., Manivasagam, T., Sankar, V., Prakash, S., Muthusamy, R., Krishnamurti, A., & Surendran, S. (2009). Withania somnifera root extract improves catecholamines and physiological abnormalities seen in a Parkinson's disease model mouse. Journal of Ethnopharmacology, 125(3), 369-373.
[56] Chaudhary, G., Sharma, U., Jagannathan, N. R., & Gupta, Y. K. (2003). Evaluation of Withania somnifera in a middle cerebral artery occlusion model of stroke in rats. Clinical and Experimental Pharmacology and Physiology, 30(5- 6), 399-404.

[57] Raghavan, A., & Shah, Z. A. (2015). Withania somnifera improves ischemic stroke outcomes by attenuating PARP1-AIF-mediated caspase-independent apoptosis. Molecular neurobiology, 52(3), 1093-1105.
[58] Kennedy, D. O., & Wightman, E. L. (2011). Herbal extracts and phytochemicals: plant secondary metabolites and the enhancement of human brain function. Advances in Nutrition, 2(1), 32-50.
[59] Khan, O. A., Ranson, M., Michael, M., Olver, I., Levitt, N. C., Mortimer, P., et al. (2008). A phase II trial of lomeguatrib and temozolomide in metastatic colorectal cancer. British journal of cancer, 98(10), 1614-1618.
[60] Quiros, S., Roos, W. P., & Kaina, B. (2010). Processing of O6-methylguanine into DNA double-strand breaks requires two rounds of replication whereas apoptosis is also induced in subsequent cell cycles. Cell cycle, 9(1), 168-178.
[61] Roos, W. P., Batista, L. F. Z., Naumann, S. C., Wick, W., Weller, M., Menck, C. F. M., & Kaina, B. (2007). Apoptosis in malignant glioma cells triggered by the temozolomide-induced DNA lesion O6-methylguanine. Oncogene, 26(2), 186-197.
[62] Newman, R. E., Soldatenkov, V. A., Dritschilo, A., & Notario, V. (2002). Poly (ADP-ribose) polymerase turnover alterations do not contribute to PARP overexpression in Ewing's sarcoma cells. Oncology reports, 9(3), 529-532.
[63] Soldatenkov, V. A., Albor, A., Patel, B. K., Dreszer, R., Dritschilo, A., & Notario, V. (1999). Regulation of the human poly (ADP-ribose) polymerase promoter by the ETS transcription factor. Oncogene, 18(27), 3954-3962.
[64] Salmas, R.E., Unlu, A., Yurtsever, M., Noskov, S.Y. and Durdagi, S. (2016). In silico investigation of PARP-1 catalytic domains in holo and apo states for the design of high-affinity PARP-1 inhibitors. Journal of enzyme inhibition and medicinal chemistry, 31(1), 112-120.
[65] Ekins, S., Mestres, J., & Testa, B. (2007). In silico pharmacology for drug discovery: methods for virtual ligand screening and profiling. British journal of pharmacology, 152(1), 9-20.